PALEONTOLOGY

The oldest mineralized bryozoan? A possible palaeostomate in the lower Cambrian of Nevada, USA

Sara B. Pruss[1]*, Lexie Leeser[1], Emily F. Smith[2], Andrey Yu. Zhuravlev[3], Paul D. Taylor[4]

All skeletal marine invertebrate phyla appeared during the Cambrian explosion, except for Bryozoa with mineralized skeletons, which first appear in the Early Ordovician. However, the skeletal diversity of Early Ordovician bryozoans suggests a preceding interval of diversification. We report a possible earliest occurrence of palaeostomate bryozoans in limestones of the Cambrian Age 4 Harkless Formation, western United States. Following recent interpretations of the early Cambrian Protomelission as a soft-bodied bryozoan, our findings add to the evidence of early Cambrian roots for the Bryozoa. The Harkless fossils resemble some esthonioporate and cystoporate bryozoans, showing a radiating pattern of densely packed tubes of the same diameter and cross-sectional shape. Further, they show partitioning of new individuals from parent tubes through the formation of a separate wall, a characteristic of interzooecial budding in bryozoans. If confirmed as bryozoans, these fossils would push back the appearance of mineralized skeletons in this phylum by ~30 million years and impact interpretations of their evolution.

INTRODUCTION

Here, we describe and interpret newly found organisms of the lower Cambrian Age 4 Harkless Formation near Gold Point, Nevada. These fossils exhibit a rigid modular calcitic structure of multiple, densely packed subparallel tubes that resemble the zooidal skeletons of some early palaeostomate bryozoans. If confirmed as bryozoans, then the Harkless fossils would represent the oldest bryozoans with calcareous skeletons, predating the previously known earliest occurrence by tens of millions of years. A phosphatized soft-bodied bryozoan, *Protomelission gatehousei*, has recently been recognized in Cambrian Age 3 sections from Australia and South China (*1*). The oldest previously accepted skeletal bryozoans occur in the Lower Ordovician (lower Tremadocian) of China from the lower Nantzinkuan Formation (*2*, *3*), with a less widely accepted first occurrence in the upper Cambrian Tiñu Formation of Mexico (*4*–*6*). While the Harkless bryomorph fossils resemble other problematic Cambrian fossils, such as *Bija*, their features most closely align with palaeostomate bryozoans.

The early Cambrian is marked by an unprecedented radiation of organisms (*7*), including the first to make robust skeletons, such as the archaeocyathan sponges [e.g., (*8*, *9*)]. The onset of animal reef building during this time is global and widespread, beginning in stage 2 (Tommotian) and continuing until the late early Cambrian extinction of archaeocyathan reefs [e.g., (*10*, *11*)]. Archaeocyathan reefs not only represent complex ecosystems (*8*, *9*, *12*, *13*) but may also have created ideal settings for other skeletal organisms like chancelloriides (*14*, *15*) and coralomorphs, including the enigmatic coral-like organism known as *Harklessia yuenglingensis* that has been found within and adjacent to archaeocyathan reefs of the Harkless Formation in Esmeralda County, Nevada (*16*, *17*).

Archaeocyathan reefs of the Harkless Formation in the western United States represent the last episode of animal reef building in the early Cambrian in western Laurentia (*9*, *15*). Although their demise may not be synchronous with the extinction of archaeocyaths globally, it does represent a local extirpation, although carbonate-rich subtidal settings persist in overlying strata, with scattered occurrences of putative archaeocyaths (*18*). In the ~20 m of the beds overlying these last archaeocyathan reefs, constrained to upper Series 2 of the Cambrian (*19*), several examples of unusual organisms in carbonate facies have been observed in thin sections.

RESULTS

Field observations

The youngest archaeocyathan reef bed of the Harkless Formation is exposed laterally in fault blocks in the hills to the northeast of Gold Point. The reefs are patchy and visible in only a few exposures of the upper Harkless (*15*, *20*), but reef talus is often present in beds where the reefs are not exposed. At GPS-4 of Pruss *et al.* (*15*), a reef talus bed is exposed and is overlain by ~10 m of sandstones. The base of our section begins above the sandstones with <1-m-thick limestone beds interbedded with siltstone (0 to 10 m) (Fig. 1); in the field, these appear as alternating rust brown/orange siltstones and bluish limestone beds (Fig. 2). The limestone facies here consist of ooid- and quartz-rich limestone. The middle of our measured section, from 10 to ~22 m, is composed of interbedded fossiliferous silty limestone with poorly exposed siltstone and shale, as well as oolitic and fine-grained carbonate, both containing rounded quartz grains. The top of the exposure is characterized by tabular intraclastic limestone, with clasts up to a decimeter in size.

The bryomorph fossils described here were first identified in the field as clasts in fossil packstones. In hand specimens, they were visible in three samples from section GPS-4 (GPS-4 7.85, GPS-4 15.45, and GPS-4 23.52) (see Fig. 1). Both transverse and longitudinal sections through the fossils are evident on cut slabs (Fig. 3). The bryomorph fossils consist of dark gray tubes infilled with paler-colored carbonate cement. Transverse views reveal clusters of subcircular to slightly polygonal tubes; longitudinal views show that the tubes are hollow and lack internal partitions (e.g., septa, tabulae, or diaphragms) and that the organisms grew in diameter by adding new tubes and lengthening existing tubes.

[1]Department of Geosciences, Smith College, Northampton, MA 01062, USA. [2]Department of Earth and Planetary Sciences, Johns Hopkins University, Baltimore, MD 21218, USA. [3]Division of Biological Evolution, Biological Faculty, Lomonosov Moscow State University, Moscow 119991, Russia. [4]Department of Earth Sciences, London Natural History Museum, Cromwell Road, London SW7 5BD, UK.
*Corresponding author. Email: spruss@smith.edu

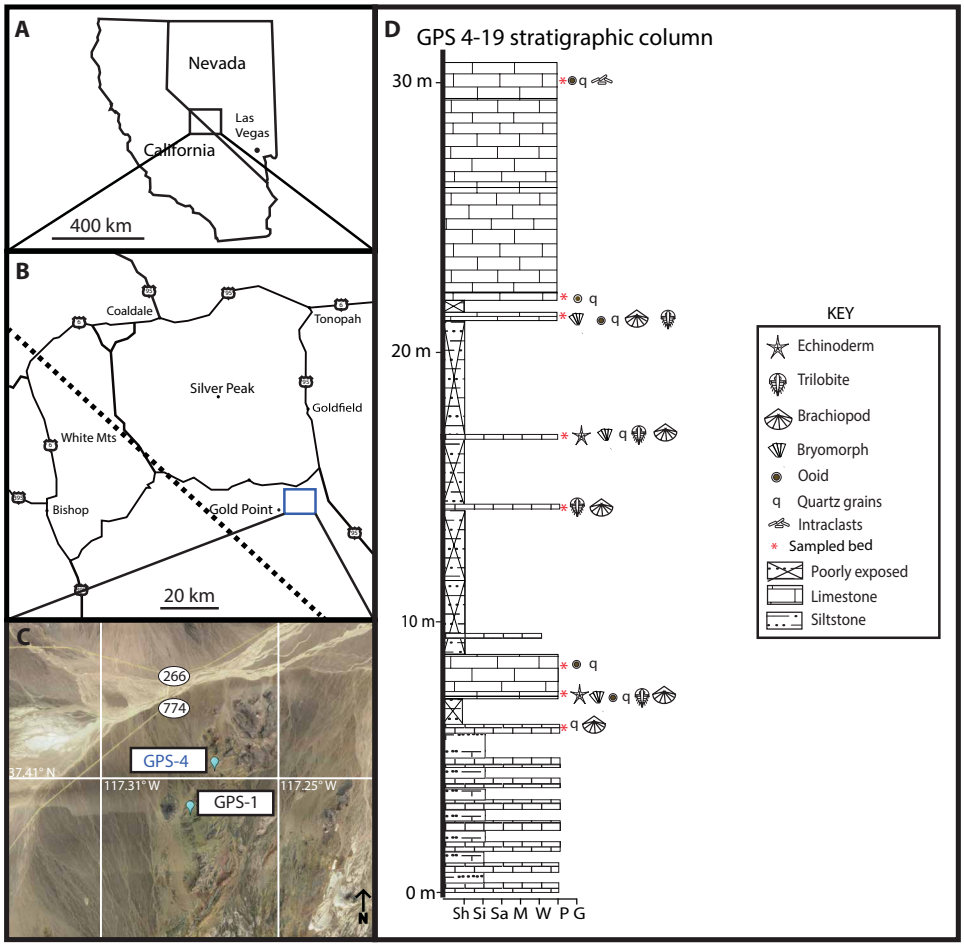

Fig. 1. Locality map and stratigraphic column. (**A**) Map of California and Nevada, western United States. (**B**) Inset from (A) shows the location of study area outside of Gold Point. (**C**) Inset from (B) shows the locations of the Harkless Formation sampled near Gold Point, Nevada, at localities GPS-1 and GPS-4 (*15*) (GPS-1: 37°24′14.17″ N, 117°16′44.53″ W; GPS-4: 37°24′44.72″ N, 117°16′35.46″ W). (**D**) Stratigraphic column of upper Harkless section containing bryomorph fossils, measured in meters (m). At the base of the column, lithologies are indicated (sh, shale; si, siltstone; sa, sandstone; m, mudstone; w, wackestone; p, packstone; g, grainstone). Mts, Mountains.

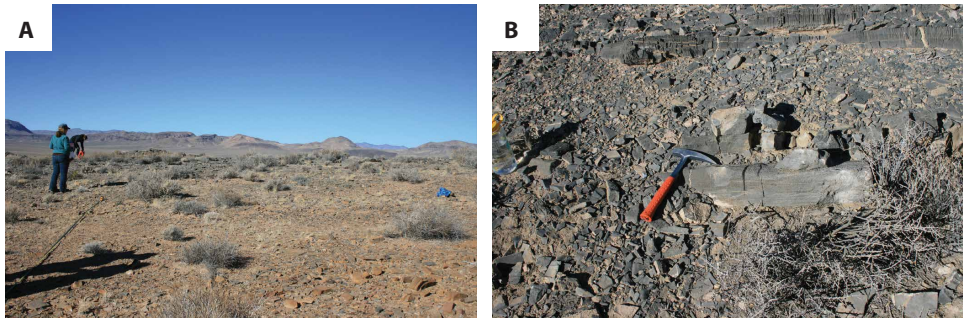

Fig. 2. Outcrop photographs. (**A**) Field photographs show poorly exposed outcrop in upper Harkless. (**B**) Thin limestone beds preserving bryomorph fossils in a dominantly recessive siliciclastic section. Hammer is ~30 cm.

Thin section observations

The bryomorph fossils were found in 21 thin sections from three stratigraphic horizons (some fossils were found in talus) at GPS-4. A subset of exceptional examples is shown in Fig. 4. GPS-1 had only one fossil-bearing stratigraphic interval. Only 3 of the 21 thin sections with these organisms were from GPS-1; the bryomorph fossils were much more prevalent in samples from GPS-4. Thin sections with the bryomorph fossils also contain ooids, quartz grains, and other invertebrate fossils including trilobite fragments, brachiopod valves, echinoderm plates, and *Salterella* conchs. Fossils were found in

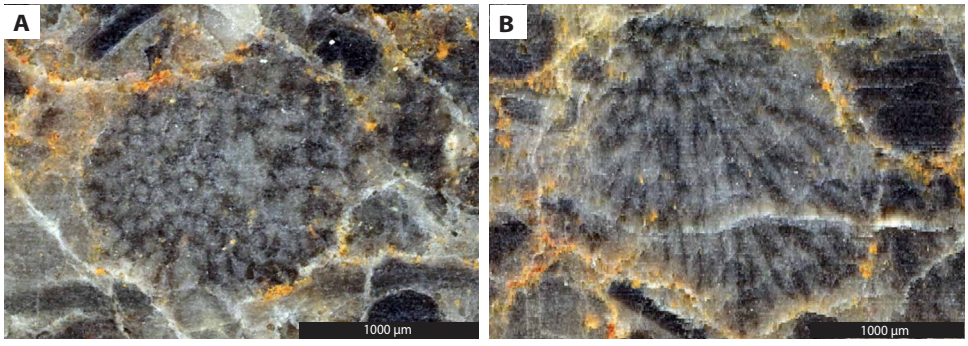

Fig. 3. Hand sample images. Cut slabs of bryomorph fossils. (**A**) Cross-sectional view showing round individual tubes. (**B**) Longitudinal cut through organism showing growth form.

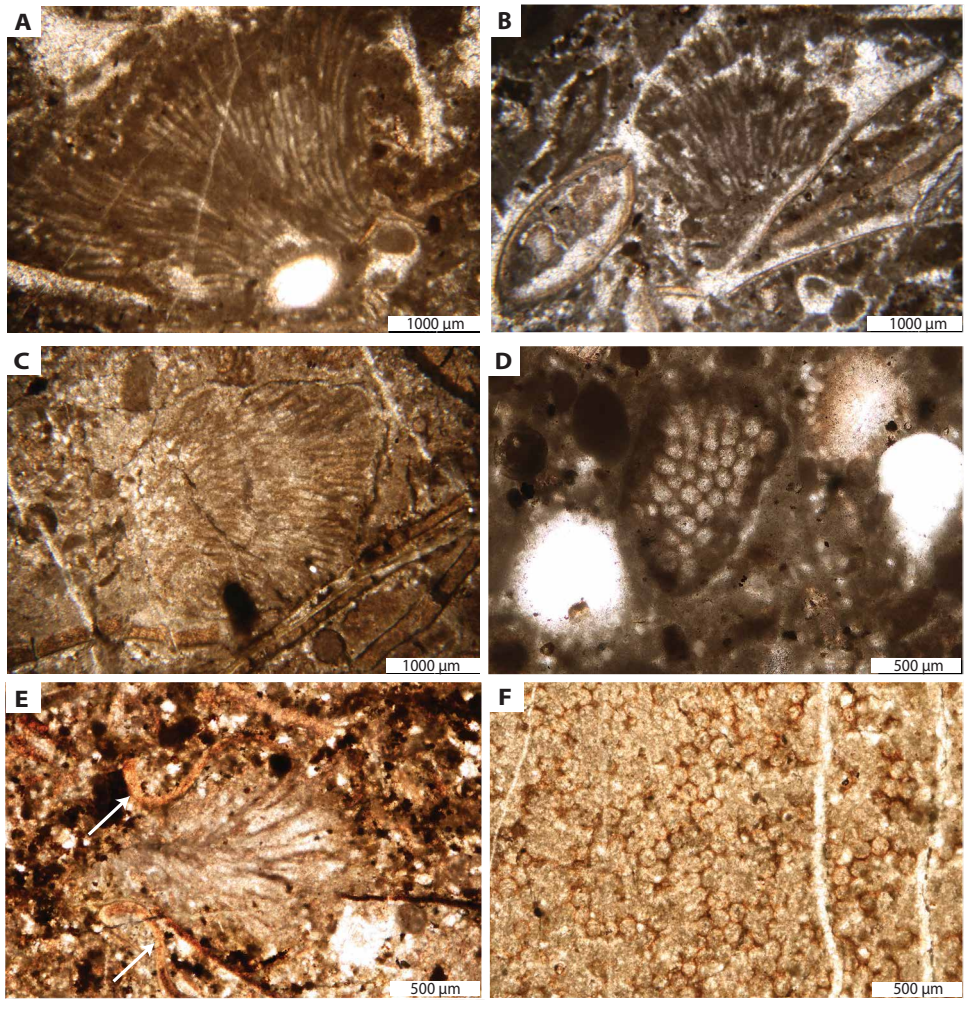

Fig. 4. Thin section images of bryomorph fossils. (**A** and **B**) Longitudinal sections of the fossils, showing a site of attachment at the base of the organism. (**C**) Dissolution around the edge of the fossil and its placement in the sediment as a clast, not in life position. (**D**) Horizontal cross sections showing subcircular individual tubes through organism. (**E**) Organism and tubes branching from the center; arrows indicate trilobite fragments. (**F**) Cross-sectional network of subcircular tubes. The preservation is variable across the organism, so not all tubes are visible.

samples between 8 and 24 m from the base of the section at GPS-4 (Fig. 1D). They were absent in fine-grained carbonate samples.

The orientation of the Harkless bryomorph fossils in our thin sections—which were cut perpendicular to bedding—varies, with transverse, oblique, and longitudinal cuts all present. Some of the fossils seen in thin section appear nearly or entirely whole (Fig. 4), but most are fragments. Sometimes, they appear attached to quartz grains or skeletal fragments (Fig. 4, A and B), and occasionally,

individual fossils show evidence of erosion or dissolution around their edges (Fig. 4C). In thin section, the fossils form compact calcareous masses comprising long tubes of relatively uniform diameter arranged radially or in a fan. Individual tubes widen slightly in a distal direction toward the edges of the fossils (Fig. 5). The width of individual specimens ranges from ~700 to ~5500 μm. Each tube has a width of 40 to 109 μm (Table 1 and Fig. 4). Measured lengths of tubes range from ~1000 to ~3000 μm, but because most of the cuts were not perpendicular to the long axis of the tubes, these measurements are underestimates of their true lengths. The thickness of the microgranular skeletal walls ranges from 17 to 52 μm (Table 1).

In addition, each bryomorph fossil, made up of numerous individual tubes, shows a net increase in the number of tubes from base to tip (Table 1 and Fig. 4A). For example, one specimen has 14 tubes at the base and 94 at the top, although the width of individual tubes remains consistent throughout the entire fossil. This creates the overall fan-like morphology seen in thin sections cut parallel to the growth direction of the organism (Fig. 4). Horizontal cross sections of the tubes show that they are circular to slightly polygonal (tetra- to hexagonal) in shape (Fig. 4, D and F).

DISCUSSION

Paleoenvironment and paleoecological interpretations

Lithologies of the ~30 m of the Harkless Formation that overlie the last archaeocyathan reefs include carbonate, siltstone, and shale. Carbonates alternate between micritic laminated beds and quartz- and ooid-rich fossil packstones (Fig. 2). The packstone facies contains the bryomorph fossils, other fossils and their fragments, and ooids and rounded quartz grains. We interpret these bryomorph fossils as having been transported before deposition. In contrast, the siltstone facies is largely devoid of fossil debris. Overall, the depositional setting of this ~30-m-thick portion of the Harkless Formation is inferred to be a shallow marine environment, with episodic storms and terrigenous input.

The assemblages in which these bryomorph fossils are preserved comprise an array of organisms that hint at a diverse benthic ecosystem. The trilobites, *Salterella*, and echinoderm fragments demonstrate the presence of both motile and sessile benthic organisms, common on early Cambrian seafloors. The bryomorph fossils discussed here are occasionally preserved attached to rip-up clasts or skeletal fragments, so likely lived as sclerobionts. Some of the individual fossils showed abrasion that occurred during transport, while others have traces of probable diagenetic dissolution around their margins, but no fossils show deformation of tubes or entire individuals, suggesting that this organism produced a rigid skeleton. The paleoenvironment and preservation of these bryomorph fossils point to an originally robust skeleton that behaved as a clast when transported into this setting.

Possible affinities of the Harkless bryomorph fossils

The coralomorph *Harklessia* from the reefs and associated facies of the Harkless Formation (*16*, *17*), while tubular, shares little in common with the bryomorph fossils described here. Coralomorphs have large individual modules (corallites) that are typically >2 mm in width (*16*), an order of magnitude larger than the tubes of the organisms described here. In true modular corals, including early Cambrian forms, a median plate or midline in the corallite walls is formed, commonly representing fused epitheca of adjacent corallites, thus imparting the wall a three-layered structure (*21*, *22*). In addition, the cross-sectional shape of the corallites is distinctly noncircular, and they are irregularly shaped. Other problematic skeletal fossils associated with early archaeocyathan reefs from the western United States include *Archaeotrypa* from the underlying Poleta Formation. This organism has been suggested as a member of the Bryozoa (*23*), Echinodermata (*24*), and Mollusca (*25*), with no consensus, but the zig-zag form of the walls evident in some longitudinal sections makes a bryozoan affinity unlikely (*6*).

There are varieties of calcimicrobial fossils that have similarities to the bryomorph fossils described here. *Bija* and *Hedstroemia* are two examples of Paleozoic calcimicrobes with structures reminiscent of the fossils described here (*26*–*28*). Originally, *Bija* was described from the Verkhneynyrga Formation of the Lebed' River, Mountain Altay, southern Siberia, Russia (*29*). *Bija* has since been found from lower Cambrian (stages 2 to 4) carbonates of other Siberian areas and the South Urals, Russia (*30*–*32*) as well as from the Mackenzie Mountains of Canada (*33*), olistoliths associated with reefs in the Great Basin, Nevada, USA (*34*), erratics in King George Island, Antarctica (*35*), and the North China Platform (*36*). The lower Cambrian Qingxudong Formation within the Yutang section in the Huayuan area of western Hunan (*37*) is contemporaneous with the Age 4 Harkless Formation of Gold Point, Nevada. In the Yutang section, calcimicrobes are present in strata that overlie the youngest archaeocyathan reefs. *Hedstroemia* boundstone, one of the three types

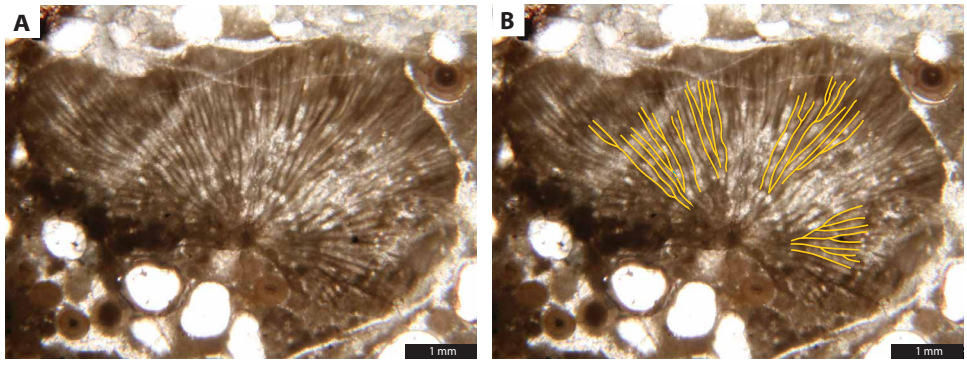

Fig. 5. Thin section images of a single bryomorph organism from the Harkless. (**A**) General fossil view. (**B**) Sketches of the branching of daughter tubes from parent tubes. Note the formation of distinct skeletal walls from the parent during budding.

Table 1. Size data from four well-preserved fossils in thin section. The number of individuals from the base to the top, size of cross sections of tubes, size of the length of tubes, and wall thickness are reported. MIN, minimum value for all tubes; MAX, maximum: MEAN, mean; STDEV, standard deviation; TOTAL, the number measured for each category; N/A, not applicable.

	Tube width (μm)	Wall thickness (μm)	Tube length (μm)	# of tubes at base	# of tubes at top
1	108	37	1766	14	94
	109	34	2655		
	52	22	1335		
	81	25	2706		
	82	31	2923		
	96	35	2160		
	85	35	2338		
	98	52	2528		
		39			
2	65	26	1935	14	37
	79	26	2238		
	63	24	2240		
	53	32	2054		
	70	19	2814		
	59				
	84				
	65				
	40				
	72				
	64				
	91				
	53				
	53				
3	63	N/A	710	13	27
	48		1200		
	48		1325		
	63		1259		
	52				
	46				
	48				
	44				
	56				
4	70	21	710	18	39
	72	30	1200		
	58	18	1325		
	69	17	1259		
	45	18			
	61				
	52				
	59				
	73				
	57				
	61				

continued on next page

	Tube width (μm)	Wall thickness (μm)	Tube length (μm)	# of tubes at base	# of tubes at top
MIN	40	17	710		
MAX	109	52	2923		
MEAN	64	29	1747		
STDEV	17	9	729		
TOTAL	42	19	21		

of reef limestone identified in the Yutang section, contains an organism similar to calcimicrobes, also described as *Bija*. Found only in float, the genus has a bush-like growth form (width of ~5 mm and height of 5 to 8 mm), with radiating tubes 80 to 160 μm in diameter (*37*). *Hedstroemia* is also reported from the overlying Mule Springs Formation in the western United States (*38*).

Bija was attributed to the corals and believed to be of middle Cambrian age (*29*, *39*), although the stratigraphic age was later corrected to the lower Cambrian (*40*), while it was subsequently noted that the extremely small sizes of the putative corallites are incompatible with a coral model (*38*). *Bija* has been compared with calcified red algae (*31*, *41*) but was assigned subsequently to the calcified cyanobacteria (*42*) because of the absence of sporangia and any other features indicative of a red alga. The cyanobacterial model compared *Bija* to calcified sheaths of extant rivulariacean cyanobacteria (*43*, *44*). Although such an interpretation of *Bija* and comparable fossils is plausible, similarly tubular compact calcified filaments with micritic microstructure have never been demonstrated in Rivulariacea or any other extant cyanobacteria (*45*–*49*). Regardless, Rivulariacea have filaments that taper at the tips, a feature sometimes tentatively reported in occurrences of *Bija* but not present in any of the >30 Harkless bryomorph fossils found to date or in type and topotype material of *Bija sibirica* Vologdin 1932 from the Verkhneynyrga Formation (Cambrian Stage 4) of Mountain Altay. There is also a notable size difference between the sheaths of modern *Rivularia* [<20 μm; e.g., (*49*, *50*)] and the tubes of the Harkless fossils (mean width of 64 μm in 42 tubes). Another similar fossil is *Solenopora*, but this genus has septa-like projections within the tubes that are typical of chaetetid sponges (*51*). The lobate cross-sectional shapes of the tubes of *Solenopora* and the flexuous walls are further differences from the Harkless bryomorph fossils.

The Harkless bryomorph fossils described in this study share morphological similarities with early palaeostomate bryozoans known from Ordovician and younger strata (*52*, *53*). In particular, they resemble some small, dome-shaped esthonioporate (*54*) and cystoporate bryozoans, which exhibit an internal radiating pattern of zooidal tubes similar in diameter and cross-sectional shape to those of the Harkless fossils. These include the Early to Middle Ordovician species of *Revalotrypa*, *Esthoniopora*, *Diplotrypa,* and *Phragmopora* described in (*55*) from Russia [see also (*56*, *57*)]. However, these bryozoans differ from the Harkless bryomorph fossils in having transverse partitioning walls (diaphragms) within the tubes, while many also have rod-like styles embedded with the walls (although we note that not all palaeostomate bryozoans share these traits). In addition, the skeletal walls of palaeostomates are typically well laminated, although some of the earliest known palaeostomate bryozoans from China have microgranular walls, probably resulting from neomorphism of originally high-Mg calcite walls (*58*), a process that may also have affected the wall fabric of the Harkless fossils destroying the primary fabric. Last, the thickness of the walls (mean 33 μm) is larger relative to tube diameter (mean 59 μm) than is typical for palaeostomate bryozoans.

One feature of the Harkless bryomorph fossils that is similar to indisputable bryozoans is the budding structure of new tubes. The bryomorph fossils generally show the partitioning of a new tube from a parent tube by the formation of a new and separate wall (Fig. 5 and Table 2). This most closely resembles the "disordered interzooecial budding pattern" recognized in trepostome bryozoans (*59*) in which each new zooecial tube originates in the corner of an existing tube with the space it occupies being partitioned from older zooecia.

Comparison with the soft-bodied bryozoan, *P. gatehousei*

P. gatehousei is a phosphatic fossil known from lower Cambrian Age 3 strata of Australia and South China. It has recently been interpreted as a soft-bodied, stem-group bryozoan (*1*), pushing back the oldest occurrence of the Bryozoa to the early Cambrian and aligning the first appearance of the phylum with other marine skeletal invertebrate phyla that first appeared in the Cambrian. This soft-bodied stem group bryozoan shares character traits with both the nonmineralized ctenostome gymnolaemates and the biomineralized stenolaemates. The Age 4 Cambrian Harkless bryomorph fossil has some character traits in common with *P. gatehousei*, such as zooids of <1 mm in diameter with a single distal opening, semiregular arrangement of zooids, and zooidal chambers separated completely by walls (Table 2). However, the Harkless bryomorph fossil has a biomineralized skeleton and tubular zooids contrasting with the box-shaped zooids of *P. gatehousei*. Together with *P. gatehousei*, the Harkless bryomorph fossil, if confirmed as a bryozoan, would add greatly to our knowledge of the early evolutionary history of the phylum.

Paleobiological implication

We report a previously undescribed fossil organism from the lower Cambrian Harkless Formation of the western United States and interpret this as possibly the earliest palaeostomate bryozoans. These fossils are rigid, comprise aggregates of tubes, and are preserved as clasts in ooid- and quartz-rich carbonate packstones ~30 m above the last stratigraphic horizon of archaeocyathan reefs in the western United States. The bryomorph fossils occasionally exhibit dissolution around the edges and show no evidence for deformation, which supports the interpretation that they were intact and rigid before transport. The size, morphology, and structure of the Harkless bryomorph fossils resembles those of *Bija* in some ways, but individual tubes of the bryomorph fossils do not taper at the tips, a

Table 2. Table showing bryozoan character traits and the presence/absence in the Harkless bryomorph fossil, after (*1*).

Bryozoan character traits	Harkless bryomorph fossil traits
Morphologically distinct founder zooid (ancestrula), typically smaller and less complex	Ancestrula unknown
Maximum surface measurement of zooid seldom exceeding 1 mm	Yes, 40–109 μm
Semiregular zooid arrangement	Yes
At least one opening (for the lophophore)	Yes
Zooid opening 50 to c. 1000 μm	Yes, 40–109 μm
Zooids overall shapes varying from box-shaped to long curved tubes	Yes, long curved tubes
Zooidal chambers separated by walls, i.e., no continuity (except for pores in some taxa)	Yes, zooidal chambers separated by walls (no pores)
Species with mineralized skeletons are calcareous	Yes, calcareous skeleton

feature tentatively ascribed to some occurrences of *Bija* and observed in modern rivulariacean cyanobacteria.

The bryomorph fossils consist of tubes that form distinct parent and daughter individuals lacking confluent cavities, a characteristic of the great majority of stenolaemate bryozoans [see (*60*) for a rare exception]. They lack the lamellar microstructure seen in most stenolaemates, although this may be artifact of neomorphism. The Harkless fossils lived during the last stages of early Cambrian reef development, appearing in close association with coralomorph-archaeocyathan reefs alongside other typical members of benthic marine ecosystems of the Cambrian. We interpret these as possible bryozoans that appeared during the early Cambrian when environmental and ecological conditions were conducive to skeleton building.

Confirmation of their palaeostomate bryozoan affinity, which could come from the finding of early growth stages with an ancestrula (founding zooid) having a bulb-like origin (protoecium), would imply a major gap during the later Cambrian in the fossil record of calcified bryozoans and prompt a reconsideration of stenolaemate bryozoan phylogeny. Other future areas for study include a more detailed comparison of Harkless bryomorph fossils with specimens of *Bija* and other early palaeostomates, including some analysis of the organism's skeletal crystal structure. Additional exploration of the upper Harkless Formation may also yield a different taphonomic window of preservation for these fossils that could provide new morphological information.

MATERIALS AND METHODS

The Upper Harkless Formation near Gold Point was sampled extensively, with sampling focused on lenticular beds of ooid- and quartz-rich carbonates overlying the last archaeocyathan reefs of the Harkless Formation (*15*). At section GPS-4, ~34 m of strata known to contain the bryomorph fossils were measured, described, and sampled at meter scale wherever exposure permitted. In addition, five samples from similar facies at GPS-1 were collected. In total, 28 samples were collected from in situ facies, and 10 samples were taken from talus and made into 43 thin sections (for some samples, two thin sections were made). More than 30 of these fossils were found under a petrographic microscope in thin section, showing variable sizes and orientations. The fossils are reasonably common in thin sections of the fossiliferous and oolitic packstone, where they exist as clasts. In thin section, four characteristics of the tubular fossils were measured: number of individual tubes from the base to the top, the length and width of the tubes, and the skeletal wall thickness (Table 1).

REFERENCES AND NOTES

1. Z. Z. Zhang, J. Ma, P. D. Taylor, L. C. Strotz, S. M. Jacquet, C. B. Skovsted, F. Chen, J. Han, G. A. Brock, Fossil evidence unveils an early Cambrian origin for Bryozoa. *Nature* 599, 251–255 (2021.
2. P. D. Taylor, A. Ernst, in *The Great Ordovician Biodiversification Event* (Columbia Univ. Press, 2004), pp. 147–156.
3. J. Ma, P. D. Taylor, F. Xia, R. Zhan, The oldest known bryozoan: *Prophyllodictya* (Cryptostomata) from the lower Tremadocian (Lower Ordovician) of Liujiachang, south-western Hubei, central China. *Palaeontology* **58**, 925–934 (2015).
4. E. Landing, A. English, J. D. Keppie, Cambrian origin of all skeletalized metazoan phyla—Discovery of Earth's oldest bryozoans (Upper Cambrian, southern Mexico). *Geology* **38**, 547–550 (2010).
5. E. Landing, J. B. Antcliffe, M. D. Brasier, A. B. English, Distinguishing Earth's oldest known bryozoan (*Pywackia*, late Cambrian) from pennatulacean octocorals (Mesozoic–Recent). *J. Paleo.* **89**, 292–317 (2015).
6. P. D. Taylor, B. Berning, M. A. Wilson, Reinterpretation of the Cambrian 'bryozoan' *Pywackia* as an octocoral. *J. Paleo.* **87**, 984–990 (2013).
7. D. H. Erwin, J. W. Valentine, *The Cambrian Explosion* (Roberts and Company, 2013).
8. A. Yu. Zhuravlev, Reef ecosystem recovery after the Early Cambrian extinction, *Biotic Recovery from Mass Extinction Events* (Geological Society of London, 1996), vol. 102, pp., 79–96; https://doi.org/10.1144/GSL.SP.1996.001.01.06.
9. S. M. Rowland, M. Hicks, The early Cambrian experiment in reef-building by metazoans. *Paleontol. Soc. Pap.* **10**, 107–130 (2004).
10. F. Debrenne, Morphogenèse et systématique des Archaeocyatha (Spongiaires, Cambrien inférieur). *Geobios* **24**, 217–222 (1991).
11. A. Y. Zhuravlev, R. A. Wood, Anoxia as the cause of the mid-Early Cambrian (Botomian) extinction event. *Geology* **24**, 311–314 (1996).
12. S. B. Pruss, H. Clemente, M. LaFlamme, Early (Series 2) Cambrian archaeocyathan reefs of southern Labrador as a locus for skeletal carbonate production. *Lethaia* **45**, 401–410 (2012).
13. J. R. Creveling, D. Fernández-Remolar, M. Rodríguez-Martínez, S. Menéndez, K. D. Bergmann, B. C. Gill, J. Abelson, R. Amils, B. L. Ehlmann, D. C. García-Bellido, J. P. Grotzinger, C. Hallmann, K. M. Stack, A. H. Knoll, Geobiology of a lower Cambrian carbonate platform, Pedroche Formation, Ossa Morena Zone, Spain. *Palaeogeogr. Palaeoclimatol. Palaeoecol.* **386**, 459–478 (2013).
14. M. Savarese, P. W. Signor, New archaeocyathan occurrences in the upper Harkless Formation (Lower Cambrian of western Nevada). *J. Paleo.* **63**, 539–549 (1989).
15. S. B. Pruss, E. F. Smith, O. Leadbetter, R. Z. Nolan, M. Hicks, D. A. Fike, Palaeoecology of the archaeocyathan reefs from the lower Cambrian Harkless Formation, southern Nevada, western United States and carbon isotopic evidence for their demise. *Palaeogeogr. Palaeoclimatol. Palaeoecol.* **536**, 109389 (2019).
16. M. Hicks, A new genus of Early Cambrian coral in Esmeralda County, southwestern Nevada. *J. Paleo.* **80**, 609–615 (2006).
17. D. R. Cordie, S. Q. Dornbos, P. J. Marenco, Increase in carbonate contribution from framework-building metazoans through early Cambrian reefs of the Western Basin and Range, USA. *Palaios* **34**, 159–174 (2019).
18. A. R. Palmer, S. M. Rowland, Day 1: Early Cambrian Stratigraphy and Paleontology, Southern Great Basin, California-Nevada. *Cambrian and Early Ordovician Stratigraphy and Paleontology of the Basin and Range Province, Western United States: Las Vegas, Nevada to Salt Lake City, Utah, July 1–7, 1989*, vol. 125 (American Geophysical Union ,1989), pp. 17–27.
19. M. Webster, J. S. Hollingsworth, F. A. Sundberg, J. R. Foster, Stops 7A, 7B, and 7C, Upper Dyeran litho-and biostratigraphy of the Split Mountain area, Nevada, in *Cambrian Stratigraphy and Paleontology of Northern Arizona and Southern Nevada*, J. S. Hollingsworth, F. A. Sundberg, J. R. Foster, Eds. (Museum of Northern Arizona Bulletin, 2011), vol. 67, pp. 236–246.
20. S. M. Rowland, L. K. Oliver, M. Hicks, E. M. Duebendorfer, E. I. Smith, Ediacaran and early Cambrian reefs of Esmeralda County, Nevada: Non-congruent communities within

congruent ecosystems across the Neoproterozoic–Paleozoic boundary, in *Field Guide to Plutons, Volcanoes, Faults, Reefs, Dinosaurs, and Possible Glaciation in Selected Areas of Arizona, California, and Nevada: Geological Society of America Field Guide*, E. M. Duebendorfer, E. I. Smith, Eds. (The Geological Society of America, 2008), vol. 11, pp, 83–100.
21. C. T. Scrutton, The Palaeozoic corals, I: Origins and relationships. *Proc. Yorkshire Geol. Soc.* **51**, 177–208 (1997).
22. M. Fuller, R. Jenkins, Reef corals from the lower Cambrian of the Flinders ranges, South Australia. *Palaeontology* **50**, 961–980 (2007).
23. M. A. Fritz, Cambrian bryozoa. *J. Paleontol.* **21**, 434–435 (1947).
24. D. R. Kobluk, *Archaeotrypa* Fritz, 1947 (Cambrian, Problematica) reinterpreted. *Can. J. Earth Sci.* **21**, 1343–1348 (1984).
25. S. M. Rowland, Earliest cavity-dwelling organisms (coelobionts), Lower Cambrian Poleta Formation, Nevada: Discussion. *Can. J. Earth Sci.* **20**, 1348–1349 (1983).
26. L. Liu, Y. Wu, H. Yang, R. Riding, Ordovician calcified cyanobacteria and associated microfossils from the Tarim Basin, Northwest China: Systematics and significance. *J. Syst. Palaeontol.* **14**, 183–210 (2016).
27. L. Liu, Y. Wu, H. Jiang, N. Wu, L. Jia, Paleoenvironmental distribution of Ordovician calcimicrobial associations in the Tarim Basin, Northwest China. *Palaios* **32**, 462–489 (2017).
28. L. Liu, L. Liang, Y. Wu, X. Zhou, L. Jia, R. Riding, Ordovician cyanobacterial calcification: A marine fossil proxy for atmospheric CO_2. *Earth Planet. Sci. Lett.* **530**, 115950 (2020).
29. A. G. Vologdin, Archaeocyaths of Siberia. Fauna of the Cambrian Limestones of the Altay (Gosudarstvennoe Nauchno-Tekhnicheskoe Geologo-Razvedochnoe Izdatel'stvo, 1932), vol. 2.
30. A. G. Vologdin, Archaeocyaths and algae of the Cambrian of the Baykal Highlands. *Paleontologicheskiy Institut, Akademiya Nauk SSSR, Trudy* **93**, 1–118 (1962.
31. K. B. Korde, *Vodorosli kembriya* (*Cambrian Algae*) (Nauka, Moscow, 1973).
32. V. A. Luchinina, Calcareous algae in Cambrian organogenous buildups of the Mana Depression. *Inst. Geologii i Geofiziki, Sibirskoe Otdelenie, Akad. Nauk SSSR, Trudy.* **669**, 77–85 (1986).
33. L. G. Voronova, N. A. Drozdova, N. V. Esakova, E. A. Zhegallo, A. Y. Zhuravlev, A. Y. Rozanov, T. A. Sayutina, G. T. Ushatinskaya, Lower Cambrian fossils of the Mackenzie Mountains (Canada). *Paleontologicheskiy Inst., Akad. Nauk SSSR, Trudy.* **224**, 1–88 (1987).
34. F. Debrenne, A. Gandin, R. A. Gangloff, Analyse sédimentologique et paléontologie de calcaires organogènes du Cambrien inférieur de Battle Mountain (Nevada, U.S.A.). *Annal. Paléontol.* **76**, 73–79 (1990).
35. R. Wrona, A. Y. Zhuravlev, Early Cambrian archaeocyaths from glacial erratics of King George Island (South Shetland Islands), Antarctica. *Palaeontol. Pol.* **55**, 10–36 (1996).
36. J.-H. Lee, H. S. Lee, J. Chen, J. Woo, S. K. Chough, Calcified microbial reefs in Cambrian Series 2, North China Platform: Implications for the evolution of Cambrian calcified microbes. *Palaeogeogr. Palaeoclimatol. Palaeoecol.* **403**, 30–42 (2014).
37. N. Adachi, Y. Ezaki, J. Liu, The late early Cambrian microbial reefs immediately after the demise of archaeocyathan reefs, Hunan Province, South China. *Palaeogeogr. Palaeoclimatol. Palaeoecol.* **407**, 45–55 (2014).
38. D. R. Cordie, S. Q. Dornbos, P. J. Marenco, Evidence for a local reef eclipse in a shallow marine carbonate environment following the regional extinction of archaeocyaths in Laurentia (Stage 4, Cambrian). *Facies* **66**, 1–20 (2020).
39. A. G. Vologdin, An Upper Cambrian coenosis of Archaeocythidae corals in the Tannu- Ola Mountain Range, Tuva. *Dokl. Akad. Nauk SSSR* **129**, 670 (1959).
40. V. V. Menner, N. V. Pokrovskaya, A. Y. Rozanov, The 'Upper Cambrian'archaeocyathid-coral assemblage in the Tannu-Ola Range (Tuva). *Izvestiya Akad. Nauk SSSR.* **7**, 99–100 (1960).
41. L. G. Voronova, E. P. Radionova, Palaeozoic algae and microphytolites. *Geologicheskiy Inst. Akad. Nauk SSSR, Trudy.* **294**, 1–220 (1976).
42. V. A. Luchinina, *Paleoalgological characteristics of the Early Cambrian of the Siberian Platform*, (Siberian Branch of Russian Academy of Sciences, Institute of Geology and Geophysics, 1975).
43. R. Riding, in *Calcareous Algae and Stromatolites* (Springer, 1991), pp. 305–334.
44. R. Riding, J. Fan, Ordovician calcified algae and cyanobacteria, northern Tarim Basin Subsurface, China. *Palaeontology* **44**, 783–810 (2001).
45. R. Riding, in *Fossil Algae* (Springer, 1977), pp. 202–211.
46. A. Pentecost, J. F. Talling, Growth and calcification of the freshwater cyanobacterium *Rivularia haematites*. *Proc. R. Soc. Biol. Sci.* **232**, 125–136 (1987).
47. M. U. Merz, The biology of carbonate precipitation by cyanobacteria. *Facies* **26**, 81–101 (1992).
48. N. Planavsky, R. P. Reid, T. W. Lyons, K. L. Myshrall, P. T. Visscher, Formation and diagenesis of modern marine calcified cyanobacteria. *Geobiology* **7**, 566–576 (2009).
49. K. Benzerara, F. Skouri-Panet, J. Li, C. Férard, M. Gugger, T. Laurent, E. Couradeau, M. Ragon, J. Cosmidis, N. Menguy, I. Margaret-Oliver, R. Tavera, P. López-García, D. Moreira, Intracellular Ca-carbonate biomineralization is widespread in cyanobacteria. *Proc. Natl. Acad. Sci. U.S.A.* **111**, 10933–10938 (2014).
50. A. Pentecost, U. Franke, Photosynthesis and calcification of the stromatolitic freshwater *cyanobacteriumRivularia*. *Eur. J. Phycol.* **45**, 345–353 (2010).
51. R. Riding, *Solenopora* is a chaetetid sponge, not an alga. *Palaeontology* **47**, 117–122 (2004).
52. P. D. Taylor, *Bryozoan Paleobiology* (John Wiley & Sons, 2020).
53. A. Ernst, in *Phylum Bryozoa*, T. Schwaha, Ed. (De Gruyter, 2020); https://doi.org/10.1515/9783110586312-002, pp. 11–56.
54. J.-Y. Ma, C. J. Buttler, P. D. Taylor, Cladistic analysis of the 'trepostome' Suborder Esthonioporina and the systematics of Palaeozoic bryozoans. *Stud. Trentini Sci. Natur.* **94**, 153–161 (2014).
55. A. V. Koromyslova, Bryozoans of the Latorp and Volkhov horizons (Lower-Middle Ordovician) of the Leningrad region. *Paleontol. J.* **45**, 887–980 (2011).
56. A. Ernst, O. K. Bogolepova, B. Hubmann, E. Y. U. Golubkova, A. P. Gubanov, *Dianulites* (Trepostomata, Bryozoa) from the Early Ordovician of Severnaya Zemlya, Arctic Russia. *Geol. Mag.* **151**, 328–338 (2014).
57. P. V. Fedorov, A. V. Koromyslova, S. O. Martha, The oldest bryozoans of Baltoscandia from the lowermost Floian (Ordovician) of north-western Russia: Two new rare, small and simple species of *Revalotrypidae*. *PalZ* **91**, 353–373 (2017).
58. J.-Y. Ma, P. D. Taylor, F.-S. Xia, New observations on the skeletons of the earliest bryozoans from the Fenhsiang Formation (Tremadocian, Lower Ordovician), Yichang, China. *Palaeoworld* **23**, 25–30 (2014).
59. F. K. McKinney, Autozooecial budding patterns in dendroid Paleozoic bryozoans. *J. Paleontol.* **51**, 303–329 (1977).
60. J.-Y. Ma, P. D. Taylor, C. J. Buttler, Unusual compound zooecia in the trepostome bryozoan *Eostenopora* from the Devonian of Guizhou, China. *Palaeoworld* **28**, 289–294 (2019).

Acknowledgments: S.B.P. thanks R. Nolan, O. Leadbetter, and A. Trossen for initial work on this project. We acknowledge the Smith College Desert Southwest class of 2018 and J. Loveless for field sampling assistance. We acknowledge BLM Paleontological Resources Use Permit no. N-94103 for our Harkless collections. We acknowledge and thank the three reviewers who offered comments and helped us strengthen our manuscript. **Funding:** This work was supported by the Smith College Geosciences Schalk Fund. **Author contributions:** Discovery: S.B.P., E.F.S., and L.L. Methodology: S.B.P., E.F.S., L.L., A.Y.Z., and P.D.T. Investigation: S.B.P. and L.L. Writing—original draft: S.B.P., A.Y.Z., L.L., and P.D.T. Writing—review and editing: S.B.P., E.F.S., L.L., A.Y.Z., and P.D.T. **Competing interests:** The authors declare that they have no competing interests. **Data and materials availability:** All data needed to evaluate the conclusions in the paper are present in the paper and/or the Supplementary Materials.

Submitted 4 November 2021
Accepted 3 March 2022
Published 20 April 2022
10.1126/sciadv.abm8465

ScienceAdvances

The oldest mineralized bryozoan? A possible palaeostomate in the lower Cambrian of Nevada, USA

Sara B. PrussLexie LeeserEmily F. SmithAndrey Yu. ZhuravlevPaul D. Taylor

Sci. Adv., 8 (16), eabm8465. • DOI: 10.1126/sciadv.abm8465